Pre-clinical characterization of ISB 1342, a CD38xCD3 T-cell engager for relapsed/refractory multiple myeloma

Blandine Pouleau, Carole Estoppey, Perrine Suere, Emilie Nallet, Amélie Laurendon, Thierry Monney, Daniela Pais Ferreira, Adam Drake, Laura Carretero-Iglesia, Julie Macoin, et al.

Pre-clinical characterization of ISB 1342, a CD38xCD3 T-cell engager for relapsed/refractory multiple myeloma

Blandine Pouleau[1#], Carole Estoppey[2#], Perrine Suere[1], Emilie Nallet[1] Amélie Laurendon[2], Thierry Monney[2], Daniela Pais[1], Adam Drake[1], Laura Carretero-Iglesia[1], Julie Macoin[1], Jérémy Berret[1], Maria Pihlgren[1], Marie-Agnès Doucey[1], Girish S. Gudi[3], Vinu Menon[3], Venkatesha Udupa[4], Abhishek Maiti[5], Gautam Borthakur[5], Ankita Srivastava[2], Stanislas Blein[2], M. Lamine Mbow[1], Thomas Matthes[6], Zeynep Kaya[7], Claire M. Edwards[7], James R. Edwards[7], Emmanuelle Menoret[8, 9], Charlotte Kervoëlen[8, 9], Catherine Pellat-Deceunynck[8,10], Philippe Moreau[8,10,11], Eugene Zhukovsky[1], Mario Perro[1*+], Myriam Chimen[1*].

[#/*] Equal Contribution

[1]Department of Oncology, Ichnos Sciences S.A., Biopôle Lausanne-Epalinges, Epalinges, Switzerland.
[2]Department of Antibody Engineering, Ichnos Sciences S.A., Biopôle Lausanne-Epalinges, Epalinges, Switzerland.
[3]Department of Pharmacokinetics and Translational Sciences, Ichnos Sciences Inc., New York, USA.
[4]Department of Toxicology, Glenmark Pharmaceuticals Limited, Mumbai, India
[5]Department of Leukemia, The University of Texas MD Anderson Cancer Center, Houston, Texas, USA.
[6]Hematology Service, Department of Oncology and Clinical Pathology Service, Department of Diagnostics, University Hospital Geneva, 1211, Geneva, Switzerland.
[7]Nuffield Department of Orthopaedics, Rheumatology and Musculoskeletal Sciences, Botnar Institute, University of Oxford, Oxford, United Kingdom.
[8]Nantes Université, Inserm, CNRS, Université d'Angers, CRCI2NA, Nantes, France
[9]Therassay core facility, Onco-Hematology department, Capacités, Nantes Université, Nantes, France.
[10]SIRIC ILIAD, Angers, Nantes, France.
[11]Service d'Hématologie Clinique, Unité d'Investigation Clinique, CHU, Nantes, France.

Corresponding Author:

Mario Perro, PhD
Ichnos Sciences S.A., Biopôle Lausanne-Epalinges, 1066 Epalinges, Switzerland.
mario.perro@ichnossciences.com
Phone: +41 21 546 06 11

Data Sharing: For original data, please contact Dr Mario Perro: mario.perro@ichnossciences.com

Running title: CD38xCD3 bispecific antibody in multiple myeloma

Scientific category: Immunobiology and Immunotherapy

Keywords: Multiple Myeloma, Bispecific, T-cell engager, daratumumab

Word counts:

Total: 4517/4000

Abstract: 221/250

Number of figures: 7

Number of tables: 1

Number of references: 69

Number of Supplementary Figures: 8

Number of Supplementary Tables: 4

Key points

- ISB 1342 exhibits potent killing of primary MM cells and MM cell lines with low sensitivity to daratumumab.
- ISB 1342 induced complete MM tumor eradication in two *in vivo* mouse models.

Abstract

Whilst treatment of multiple myeloma (MM) with daratumumab significantly extend patient lifespan, resistance to therapy is inevitable. ISB 1342 was designed to target MM cells from patients with relapsed/refractory MM (r/rMM) displaying lower sensitivity to daratumumab. ISB 1342 is a bispecific antibody with a high affinity Fab binding to CD38 on tumor cells on a different epitope than daratumumab and a detuned scFv domain affinity binding to CD3ε on T-cells, to mitigate the risk of life-threatening cytokine release syndrome, using the Bispecific Engagement by Antibodies based on the TCR (BEAT®) platform. *In vitro*, ISB 1342 efficiently killed cell lines with different levels of CD38 including those with a lower sensitivity to daratumumab. In a killing assay, wherein multiple modes of action were enabled, ISB 1342 showed higher cytotoxicity towards MM cells compared to daratumumab. This activity was retained when used in sequential or concomitant combinations with daratumumab. The efficacy of ISB 1342 was maintained in daratumumab-treated bone marrow patient samples showing lower sensitivity to daratumumab. ISB 1342 induced complete tumor control in two therapeutic mouse models, unlike daratumumab. Lastly, in cynomolgus monkeys, ISB 1342 displayed an acceptable toxicology profile. These data suggest that ISB 1342 may be an option in patients with r/rMM refractory to prior anti-CD38 bivalent monoclonal antibody therapies. It is currently developed in a phase 1 clinical study.

Introduction

Multiple myeloma (MM) is the second most common haematological malignancy worldwide, with 35,500 and 54,600 new cases anticipated in 2025 in the USA and Europe, respectively (1). The emergence of CD38-targeted therapies has significantly prolonged the survival of patients with relapsed/refractory MM (r/rMM) who were previously treated with ≥2 prior therapies. Daratumumab, a human IgG1 monoclonal antibody targeting CD38, is associated with a median overall survival (OS) of 20.1 months in patients refractory to proteasome inhibitors and immunomodulatory drugs (2,3). Mechanistically, daratumumab induces killing of MM cells via antibody-dependent phagocytosis (ADCP), complement-dependent cytotoxicity (CDC), antibody-dependent cellular cytotoxicity (ADCC) and by inducing direct apoptosis via FcγRs-mediated cross-linking (4–6). Clinical outcomes have further improved with the approval of daratumumab combinations compared to monotherapy (4,7,8). Despite such progress, most patients continue to relapse, due to multiple primary and acquired resistance mechanisms to anti-CD38 therapies (4,9,10). Amongst those mechanisms, transient down-regulation of CD38 expression on the surface of MM cells, which never fully recover expression, has been observed in patients treated with daratumumab (11).

ISB 1342 was therefore designed to be active regardless of CD38 expression and to overcome pre-existing resistance to daratumumab's many mechanisms of action. ISB 1342 was engineered using the BEAT® platform (**B**ispecific **E**ngagement by **A**ntibodies based on the **T**CR platform) (12–14) to target the cluster of differentiation (CD)3-epsilon (CD3ε) and CD38. ISB 1342 aims to treat r/rMM, by targeting and depleting $CD38^+$ MM cells via a T-cell redirected killing by crosslinking the CD3ε molecules on T-cells and the CD38 molecules on MM cells. This bridging activates T-cells in a polyclonal manner, independent of the involvement of a specific antigenic peptide presented on the major histocompatibility class (MHC) proteins or costimulatory molecules (15,16).

In this study, we evaluated the ability of ISB 1342 to kill MM cells, which model some resistance mechanisms to daratumumab in patients. We demonstrate that ISB 1342 can successfully induce the killing of MM cell lines *in vitro* and *in vivo*, as well as of primary MM cells in bone marrow aspirates (BMA) from patients previously exposed to daratumumab, whereas the latter possesses limited activity under these conditions. Studies in cynomolgus monkeys revealed an acceptable toxicology profile and supported the advancement of ISB 1342 into an ongoing Phase 1 dose-escalation clinical study in r/rMM patients.

Material and Methods

Additional detailed methods are presented in the supplemental file.

Human samples and cell lines

BMA or peripheral blood samples from MM patients were obtained from University Hospital Geneva, CHU Nantes (MYRACLE cohort **(17)**), and Oxford University Hospitals with informed consent under each site ethical approvals. Human PBMCs (hPBMC) from healthy donors and MM patients, and bone marrow mononuclear cells (BMMC) were isolated using Ficoll gradients. All cell lines were of human origin (from DSMZ or Sigma-Aldrich) and cultured in the media recommended by the supplier.

Redirected lysis (RDL) assay

MM cell lines were labelled with eFluor™670 dye (2µM) or CFSE (1µM) and co-cultured for 48-72 hours with hPBMCs at an effector to target ratio (E:T) of 10:1 or 5:1 with ISB 1342 or control molecules and additional treatments (soluble CD38, dexamethasone). The MM cell killing was measured as the decrease of the remaining live target cells count after treatment (based on viability dye staining) normalized with the untreated and non-effector cells conditions. The T-cell response was measured as the proportion of live $CD8^+$T-cells expressing CD25, Ki-67 and Granzyme B/Perforin (**Supplementary Table 1, 2**).

Multiple Mode of Action Killing assay (MMoAK)

hPBMCs were co-cultured with MM cell lines previously labelled with eFluor670 (2µM) in medium containing 50%Human Serum (HS) and 100U/ml hIL-2 at E:T of 5:1 to enable ADCC, ADCP, CDC, and T-cell mediated cytotoxicity (**Figure 3F**). Co-cultures were then incubated with ISB 1342, daratumumab (Darzalex®, Janssen Biotech Inc.) or control molecules. The MM cell killing was measured as the decrease of the remaining live target cells count after treatment (based on viability dye staining) normalized with the untreated and non-effector cells conditions. The T-cell response was measured as the proportion of live $CD8^+$T-cells expressing CD25, CD69 and CD107a (**Supplementary Table 1, 2**).

Ex vivo assay on MM patient samples

Baseline phenotype analysis was performed on 0.2-0.5x10^6 BMMC and MM cell lines to assess the phenotype of MM cells and T-cells (**Supplementary Table 1**). Killing assay was performed on 0.1-0.2x10^6 BMMC treated with ISB 1342 or daratumumab in medium containing 10%HS and hIL-6 (3ng/ml) for 17-32 hours at 37°C (**Supplementary Table 2**). Tumor cell killing was calculated as the decrease of the remaining live target cell count, defined as $CD138^+$, after treatment, normalized to the untreated condition. The T-cell response was measured as the proportion of live $CD8^+$T-cells expressing CD25, CD69, and CD107a.

In vivo efficacy mouse model

The *in vivo* study was performed with 6/7-week-old immunodeficient female NSG (NOD.Cg-*Prkdc*^{scid} *Il2rg*^{tm1Wjl}/SzJ) mice (8 mice per group) from Charles River Laboratories and conducted according to the Swiss Animal Protection Law with authorization from the cantonal and federal veterinary authorities. $10x10^6$ KMS-12-BM cells were injected s.c. and $10x10^6$ hPBMC were injected intraperitoneally (i.p.). Treatments were injected i.v. 9 days after, when tumors reached an average volume of $150mm^3$ and then once (ISB 1342) or twice (daratumumab)/week, for 3 weeks. Immunoglobulins (IVIg) were injected i.v. one day before each treatment injection. When animals reached maximum tumor size (1000 mm3) prior to study endpoint, they were euthanized, and last observation carried forward (LOCF) was used. Tumor size was evaluated three times/week. For the flow-cytometry analysis, tumors were harvested 7 days after the first treatment injection and dissociated with an enzymatic cocktail from a tumor dissociation kit using a GentleMACS dissociator. Cells in suspension were filtered, red blood cells (RBC) lyzed, and stained for human immune cell infiltration and CD38 expression on tumor cells (**Supplementary Table 1**).

Studies in cynomolgus monkeys

Monkey studies were conducted at SNBL USA Ltd, an AAALAC-accredited facility. Purpose-bred (Cambodian origin), naïve male and female cynomolgus monkeys were used in the non-GLP study. The study protocol and amendments were approved by the study director and SNBL's IACUC. All procedures were performed in compliance with the SNBL SOPs. Cynomolgus monkeys (1 male and 1 female) received a single intravenous (i.v.) bolus injection at escalating doses of ISB 1342 (1, 100, and 1000 µg/kg at day 1, 29, and 57, respectively). Clinical observations and blood samples were collected for clinical pathology, cytokines, anti-drug antibody (ADA), and flow cytometry analysis of leukocyte populations (**Supplementary Table 1**). The serum concentrations of ISB 1342 were measured using an exploratory hybrid IP-LC/MS/MS method at Q2 solutions (Ithaca, USA).

Results

ISB 1342 Engineering and biophysical characterization

The anti-CD3ε scFv portion of ISB 1342 was genetically engineered by fusing the variable heavy chain and light chain domains of a humanized version of the SP34 mouse antibody via a 15-amino acid (aa) linker ($(Gly_4Ser)_3$). The resulting scFv domain is connected to the hinge region via a short 5-aa linker (Gly_4Thr). The Fab portion is based on a humanized mouse anti-human CD38 antibody, 9G7, developed by Ichnos and dubbed humanized 9G7 (h9G7). Fc receptors (FcR) expressed on human peripheral blood cells drive cytotoxic, phagocytic, and inflammatory functions (18,19). To prevent FcγR-mediated binding, which may act as an antibody sink and potentially crosslink FcγR-expressing immune cells with T-cells, and to minimize non-specific T-cell activation (in the absence of target cell engagement), two mutations, LALA (L234A/L235A, EU numbering), were introduced into the CH2 domains of ISB 1342 (**Figure 1 A**). These mutations decrease the binding of human IgG1 molecules to human FcγR (20,21). ISB 1342 interacted weakly with all FcγR compared to its Fc-competent counterpart (**Supplementary Figure 1A, B**). ISB 1342 was designed to bind to CD38 expressing tumor cells with high affinity while mitigating the risk of life-threatening cytokine release syndrome (CRS) in the clinic by detuning the affinity to CD3ε still to effective level (22). ISB 1342 binding to human CD38 and CD3εδ recombinant proteins displayed K_D of 1.1±0.15nM and 125±2.8nM, respectively, when SPR results were analyzed using the Langmuir 1:1 model (**Figure 1B and Supplementary Figure 1C**). On MM cell lines expressing different levels of CD38, such as KMS-12-BM ($CD38^+$), NCI-H929 ($CD38^{++}$) and MOLP-8 ($CD38^{+++}$), ISB 1342 affinity was higher (K_D=2.5±1.8nM on KMS-12-BM) than on human $CD3^+CD38^-$T-cells (K_D=230.4±44.8nM) (**Figure 1B, C**). ISB 1342 was designed to target an epitope different from daratumumab as shown by the non-overlapping antigen binding footprints on the 3D structure of CD38 (**Figure 1D**). The lack of competition was

confirmed by the ability of ISB 1342 to bind CD38 despite pre-incubation of CD38 with daratumumab in a biolayer interferometry assay (**Figure 1E**).

ISB 1342 induces killing of MM cell lines

We explored the ability of ISB 1342 to specifically kill MM cell lines by engaging T-cells *in vitro*, using a RDL assay with hPBMC as effectors. First, we evaluated the ability of ISB 1342 to mediate synapse formation by confocal microscopy. ISB 1342 was located and enriched at the interface between T-cells and KMS-12-BM after at least 4 hours, suggesting the formation of an immunological synapse (**Figure 2A, Supplementary Figure 2A**). Next, we evaluated whether ISB 1342 induced killing of KMS-12-BM cells compared to molecules with one or both arms replaced by null arms. ISB 1342 killed with an average half-maximal effective concentration (EC_{50}) of 1.23pM while controls did not induce sufficient killing to calculate an EC_{50} (**Figure 2B**). This killing was paired with increased expression of CD25 on $CD8^+$ (**Figure 2C**), and $CD4^+$T-cells (data not shown), elevated T-cell proliferation (Ki-67 staining), and Granzyme B and Perforin (**Figure 1D-E, Supplementary Figure 2B**). No significant increases for any of these markers were seen with control molecules. Cell staining confirmed efficient binding of ISB 1342 (**Supplementary Figure 2C**) to both cell types while controls bound at similar levels to tumor (CD38 only control) and T-cells (CD3 only control). We then evaluated potential T-cell fratricide by ISB 1342. A549 cells expressing CD38 and EGFR were targeted by a T-cell engager (TCE) with the same CD3 arm as ISB 1342 but targeting EGFR that is not expressed on T-cells and therefore not expected to induce any T-cell fratricide. In these conditions, both TCE had similar cytotoxic activity and displayed similar counts of $CD8^+CD38^+$T-cells, which suggests that ISB 1342 is not inducing T-cell fratricide (**Supplementary Figure 2D, E**). Taken together these data indicate that ISB 1342 induces co-engagement of CD38 on tumor cells and CD3ε on T-cells, mediating T-cell activation and killing of tumor cells.

We next tested whether the cytotoxicity of ISB 1342 could be influenced by soluble CD38 (sCD38), which is found in MM patients at concentrations up to 2.8ng/ml in serum (23,24). At this concentration, no effect was observed on the cytotoxicity of ISB 1342 (**Figure 2F**). MM patients undergoing treatment with TCE, often receive corticosteroids, such as dexamethasone, to treat cytokine-associated toxicities including CRS (25). Treatment with dexamethasone induced a significant reduction of ISB 1342 cytotoxicity, but no change in maximum killing (**Figure 2G**). In contrast, maximum cytokine release was reduced for TNF-α, IL-6 and IL-2 in the presence of dexamethasone (**Figure 2H**). Taken together these data support that ISB 1342-induced cytokine release may be manageable with dexamethasone, while maximum killing of tumor cells is sustained.

ISB 1342 induces potent killing of MM cells with low sensitivity to daratumumab

Nihof *et al.* show that the level of CD38 expression on patient MM cells is associated with response to daratumumab therapy (11). To explore the relative impact of CD38 expression on ISB 1342 and daratumumab activities, four cell lines with different CD38 expression levels (**Figure 3A**) were evaluated. KMS-12-BM and NCI-H929 resemble r/rMM patients with lower CD38 expression, while expression on RPMI-8226 and MOLP-8 is high. We noted reduced CDC and ADCP on KMS-12-BM and NCI-H929 compared to MOLP-8 with daratumumab (**Figure 3B, C**). However, similar ADCC levels were observed with all cell lines (**Figure 3D**). These observations indicate that KMS-12-BM and NCI-H929 indeed exhibit some resistance features of patient-derived MM cells with reduced sensitivity to daratumumab-mediated killing. With ISB 1342, similar cytotoxicity was seen for all three cell lines in a RDL assay (**Figure 3E**), suggesting that the activity of ISB 1342 does not depend on CD38 expression levels.

To evaluate the combined effect of these observations directly in a single assay, we developed a multiple mode of action killing assay (MMoAK), where ADCC, ADCP, CDC, and T-cell mediated cytotoxicity are enabled (**Figure 3F**). To achieve this, hPBMC were co-cultured with MM cells in 50% human serum as a source of complement, and interleukin-2 (hIL-2) in order to facilitate NK cell functions (26). On KMS-12-BM, NCI-H929 and RPMI8226 (CD38++++), we observed a higher cytotoxicity for ISB 1342 compared to daratumumab

(**Figure 3F-H**), notably with both a lower EC_{50} in all cell lines tested and a higher maximal killing for NCI-H929 and RPMI8226. ISB 1342 was able to kill the three cell lines at similar levels, independently of CD38 expression, and also efficiently activated T-cells in this model (**Figure 3G**, **Supplementary Figure 3A, B**).

Given the utilization of daratumumab in early lines of therapy, we then aimed to determine whether co- or pre-treatment with this drug could influence cytotoxicity of ISB 1342 *in vitro*. In a concomitant MMoAK model (**Figure 4A**), daratumumab (at pre-determined EC_{50}=0.2nM) did not influence cytotoxicity, maximum killing and T-cell activation/degranulation of ISB 1342 (**Figure 4B, C**). In the sequential treatment model (**Figure 4D**), ISB 1342 potency and T-cell activation/degranulation were also unchanged before and after pre-treatment with daratumumab (**Figure 4E, F)**. In both models, the percentage of $CD8^+CD38^+$ T-cells was higher in presence of ISB 1342 but not with daratumumab only, whereas the absolute numbers were reduced with ISB 1342 in the sequential model only (**Supplementary Figure 3C**). These results suggest that at 72 hours, in this model, T-cell viability starts reducing upon activation by ISB 1342 whereas daratumumab is not affecting T-cells. Thus, the use of ISB 1342 in daratumumab pre-treated patients following a limited wash-out period should be possible since residual daratumumab should not interfere with ISB 1342 efficacy.

ISB 1342 induces killing of primary MM cells from patients

We evaluated the activity of ISB 1342 and daratumumab in samples from patients not previously treated with daratumumab (dara-naïve), including smoldering MM, newly diagnosed MM, newly diagnosed Plasma Cell Leukemia (PCL) and patient at relapse versus patients previously treated with daratumumab (dara-exposed), including heavily treated relapsed/refractory patients (**Supplementary Table 3**). Both daratumumab and ISB 1342 achieved efficient killing of dara-naïve MM cells, while only ISB 1342 was able to achieve efficient killing of dara-exposed MM cells or a single PCL sample (with an EC50 of 77.7pM) (**Figure 5A-D**). Viability of MM cells was similar at baseline and after 18-24h in culture (**Supplementary Figure 4A, B**). Dara-exposed patients had significantly lower $CD8^+$T-cells, NK cells and monocytes/macrophages to MM cells ratio than dara-naïve patients (**Figure 5E; Supplementary Figure 4C-E**). Thus, the activity of daratumumab correlated with the ratios of NK cells and monocytes/macrophages to MM cells whereas we observed no correlation between the $CD8^+$T-cell:MM cell ratio and ISB 1342 cytotoxic activity (**Supplementary Figure 4F-H).** Counts of $CD8^+CD38^+$T-cells were slightly higher in the presence of ISB 1342 compared to daratumumab and counts of NK cells and monocytes/macrophages were not affected by daratumumab or ISB 1342 treatments (**Supplementary Figure 5A-C**), suggesting an absence of on-target off-tumor killing and T-cell fratricide under these conditions. ISB 1342 was also able to efficiently induce cytotoxicity towards tumor cells from patients with Waldenstrom macroglobulinemia and T-cell acute lymphoblastic leukemia (T-ALL) both expressing low levels of CD38 (**Supplementary Figure 5D, E**). Importantly, all patient samples, irrespective of the group considered, responded to ISB 1342 and showed an increased fraction of activated $CD4^+$ and $CD8^+$T-cells as measured by the increase in $CD25^+$ and $CD69^+$T-cells (**Figure 5F, G; Supplementary Figure 5F**).

ISB 1342 exhibits anti-tumor activity *in vivo*

We evaluated the anti-tumor activity of ISB 1342 in two mouse models. NSG mice were engrafted s.c. with KMS-12-BM and injected i.p. with hPBMC (**Figure 6A**). In this model, ISB 1342 was able to control tumor growth by day 12, whereas we detected no tumor regression with daratumumab compared to vehicle control (**Figure 6B**). Additionally, an increase in the number of tumor-infiltrating $hCD45^+$ cells and T-cell were detected specifically in mice treated with ISB 1342 on day 7 (**Figure 6C, D**), as expected from TCE mechanism of action (27–30). We also observed a substantial increase in $CD25^+$ and/or $CD69^+$ tumor infiltrating T-cells reflecting their activated status (**Figure 6E**). A second model expressing very high levels of CD38 (Daudi) showed similar tumor control for ISB 1342. In this model, daratumumab was able to induce partial control of tumor growth and no tumor control was detected with the CD3 only control (**Supplementary Figure 6**). These *in vivo* results show

that ISB 1342 tumor cell killing is triggered *in vivo* independently of CD38 expression levels unlike daratumumab.

ISB 1342 shows an adequate profile in PK/PD and safety studies

Cancer immunotherapies are often associated with toxicity and tolerability events generally caused by elevated cytokine release (31). Since CD38 is expressed on human immune cells, in particular on NK, B and myeloid cells at similar levels to KMS-12-BM MM cells (**Supplementary Figure 7A**), we therefore examined the ability of ISB 1342 to influence peripheral immune cells in a high-density PBMC assay (HD-PBMC). Indeed, this assay has been previously reported to increase the sensitivity to T-cell responses and is commonly used for evaluation of toxicity of TCE (32,33). In this assay, we did not observe any depletion of peripheral leukocytes *in vitro* compared to the untreated condition (**Supplementary Figure 7B**). In addition, we found that less ISB 1342 bound to CD38 on RBC compared to daratumumab and observed no sensitization of RBC to hemagglutination compared to positive controls (**Supplementary Figure 7C, D**). We then investigated the PD changes in peripheral leukocyte populations, cytokines levels, and ISB 1342 PK using cynomolgus monkeys injected i.v. with consecutive doses of ISB 1342. In cynomolgus monkeys, expression of CD38 on peripheral leukocytes was observed at a significantly higher level on B-cells compared to monocytes, $CD4^+$ and $CD8^+$T-cells (**Figure 7A**); and resulted in detectable levels of ISB 1342 binding to B-cells (**Figure 7B**). One male and one female cynomolgus monkeys received ISB 1342 on day 1 (1µg/kg), day 29 (100µg/kg) and day 57 (1000µg/kg). ISB 1342 induced an initial reduction in B-cell numbers following each dose compared to baseline counts, which rebounded over time but not to baseline levels (**Figure 7C**). A similar profile was observed for monocytes, however levels returned to baseline after the first two doses (**Figure 7D**). Such a transient reduction in peripheral populations could reflect re-distribution of these cells rather than depletion. The number of $CD4^+$ and particularly of $CD8^+$T-cells, including activated $CD69^+$T-cells, substantially increased above the baseline in the circulation of animals administrated with 100µg/kg, indicating T-cell activation and expansion in the periphery (**Figure 7E-H**). A substantial dose-dependent elevation in serum cytokines such as IFN-γ was also observed (**Figure 7I**). ISB 1342 serum concentration profiles followed a bi-phasic disposition with a short distribution phase, followed by a longer terminal elimination phase. The terminal elimination half-life, not confounded by anti-drug antibodies (ADA) was approximately 4.75 days (**Figure 7J**). The reduced half-life of ISB 1342 observed at 1000µg/kg may be a reflection of ADA appearance at this dose (**Table 1**). These observations were confirmed with the single dose study at 100µg/kg (**Supplementary Figure 8, Supplementary Table 4**). Overall, in this study, the dose-limiting toxicity (DLT) was considered to be the CRS and the maximum tolerated dose (MTD) was 100µg/kg using i.v. route. ISB 1342 therefore revealed the most common DLT of TCE and adequate PD and PK profiles to highlight a potential therapeutic window.

Discussion

Advancement in the therapy of MM has substantially improved with the introduction of CD38-targeted monoclonal antibodies (34,35). Daratumumab, the first approved CD38-targeting monoclonal antibody, has shown significant efficacy in MM (36) both as a single therapy (37) and as a combination (7,38,39). Despite these results, most patients relapse and become refractory to daratumumab. Though efficacious, isatuximab, the second approved anti-CD38 monoclonal antibody (40) cannot be used as salvage therapy, as it targets CD38 with a similar mode of action, and therefore will be unable to overcome escape mechanisms of daratumumab treatment (10). The use of TCE like ISB 1342, could instead be an option for these patients. The data presented here show that ISB 1342 exhibits more potent cytotoxicity than daratumumab when tested on MM cell lines with varying CD38 expression and lower sensitivity to daratumumab, on patient BMA or *in vivo*. Importantly, the potency of ISB 1342 was not affected when combined with daratumumab or in the presence of soluble CD38.

The concept of a CD38xCD3 TCE (12,41) is explored in two other disclosed programs: 1) AMG424, (Xencor and Amgen) (23); and 2) CD38xCD28xCD3 tri-specific antibody (Sanofi)

(42). AMG424 showed good killing activity both *in vitro* and *in vivo*. This TCE presents a higher affinity to CD3 (15nM in SPR) than ISB 1342, a similar affinity to CD38 (7.7nM). Unlike the observations we describe here for ISB 1342, AMG424 seems to induce significant depletion of peripheral immune cell populations both *in vitro* and *in vivo* (23). The sponsor is currently testing this candidate in the context of T-ALL and Acute Myeloid Leukemia (AML) (NCT05038644). The tri-specific CD38xCD28xCD3 may enhance the potency and persistence of T-cells by providing costimulatory signals. The reported *in vitro/in vivo* results warranted a clinical trial (NCT04401020). Another CD3xCD38 TCE was described recently and is not currently in clinical development (43). The activity of this TCE seems to depend on the expression levels of CD38 but did not induce depletion of peripheral immune cells. Despite these advantages in terms of absence of on-target off-tumor activity and the lack of dependency on CD38 levels of ISB 1342 compared to published CD3xCD38 TCEs, direct comparison of ISB 1342 to these based on published data is not straightforward without a side-by-side investigation *in vitro* and *in vivo*.

ISB 1342 was designed with the advantage that it targets a different epitope from daratumumab to avoid long wash-out periods. Indeed, a minimal washout period of 3-6 months is usually necessary with other anti-CD38 therapies targeting overlapping epitopes or with daratumumab re-treatments due to the decrease in CD38 expression and potential competition (11). This delay in treating patients can be problematic and favor the occurrence of resistant clones (44). The key resistance mechanisms described for daratumumab include: down-regulation of CD38 (11,45), increased expression of complement inhibitors (CD46, CD55, CD59) limiting CDC (11), and up-regulation of CD47, which interferes with phagocytosis (10). Here, we modelled lower sensitivity to daratumumab using cell lines displaying some of these features, and patient samples post-daratumumab therapy. In agreement with the literature, the activity of daratumumab was also influenced by the ratio of effector to MM cells in patient samples (46). However, the data presented here show that the mode of action of ISB 1342 is mediated by T-cells, making it insensitive to the features of daratumumab resistance such as up-regulation of complement inhibitors proteins or to CD47. We also show that ISB 1342 can efficiently kill MM cells regardless of CD38 expression, T-cell to MM cell ratio and recent treatment with daratumumab, providing a rationale for using ISB 1342 in patients relapsing following daratumumab treatment.

MM patients showing a T-cell exhaustion profile are more likely to develop progressive disease compared to those with less exhaustion (47). Indeed, patients undergoing autologous stem cell transplantation (ASCT) plus lenalidomide as maintenance therapy, exhibit signs of T-cell exhaustion before relapsing (48). Similar pre-clinical findings were observed in the context of TCEs. In fact, when blinatumomab was continuously administered for 28 days, T-cells developed an exhausted phenotype and could not kill target cells; while with intermittent dosing, T-cells retained their memory $TCF1^+$ phenotype and could control tumor growth in the presence of blinatumomab (49). The quality of T-cells defines the activity of TCEs. Hence, some bispecific antibodies are displaying potent cytotoxicity on primary MM mostly in the presence of heathy T-cells (50), but showing reduced activity when exhaustion was detected (51). Several preclinical studies have also shown that a combination with an anti-PD-1 antibody can enhance tumor control by a TCE (52,53). More studies are required to understand how treatment with ISB 1342 will influence T-cell phenotype in the long-term, nevertheless recent studies demonstrate that patients may benefit from a sequence of two different TCE therapies (54). With the recent approval of teclistamab (BCMA TCE, Janssen Biotech) in r/rMM patients, these findings are key to support the development of ISB 1342 in the clinic, which is likely to be administered to patients previously treated with other TCEs. Despite the development and approval of efficient BCMA-targeted-therapies, studies have characterized antigen loss, biallelic deletion on chromosome 16 encompassing the BCMA locus, point mutations, shedding and anti-drug antibodies as mechanisms of resistance to anti-BMCA therapies (55–59). Therefore, it remains essential to monitor biomarkers indicative of these mechanisms and to develop TCE against other validated antigens such as CD38, to guarantee a range of therapeutic options for patients depending on the features associated with their relapse.

TCE therapies are associated with a systemic cytokine release, which is a product of their mode of action. However, this functional cytokine release can progress into CRS, which usually requires intensive care (60–63). Mitigating CRS, while maintaining potential for a beneficial anti-tumor response, is key for TCE therapies, including ISB 1342 (64). However, risk factors such as tumor burden and co-morbidities often associated with severe CRS should be considered carefully. Corticosteroid treatment is often used to mitigate CRS in the clinic, and data shown here demonstrate that use of dexamethasone does not strongly affect ISB 1342 cytotoxicity and led to a significant reduction of CRS-associated cytokines *in vitro*. Using a priming dose or step-up dosing regimen could also mitigate CRS. Indeed, in the teclistamab trial, 40 patients received 1500µg/kg, after 60µg/kg and 300µg/kg step-up doses, and no dose-limiting toxicities were observed (65). Lastly, the use of monoclonal antibodies before injection of a TCE to reduce peripheral tumor burden, could also mitigate CRS. For instance, such an approach was tested for glofitamab (27,66), an anti-CD20 TCE, which was administered after one dose of obinutuzumab (anti-CD20 antibody, Roche). This strategy resulted in a manageable CRS while preserving strong potency (67). Whether such approaches could be used for ISB 1342 remains to be clarified in clinical trials. Although, preclinical models can assess cytokine release in response to TCE, the field lacks models that accurately predict the occurrence and intensity of CRS in humans. Thus, more studies are warranted to fully assess CRS and to design better options to efficiently mitigate it, such as JAK, mTOR and Src/Ick inhibitors currently under investigation (68).

In conclusion, ISB 1342 is a potent TCE that may be used immediately after or concomitantly with daratumumab to circumvent escape via CD38 downregulation and other mechanisms described previously. Our study suggests that ISB 1342 could elicit anti-tumor clinical responses in patients with r/rMM who have previously received daratumumab therapy. Based on this encouraging preclinical data and the differentiation from other CD38-targeting therapeutics used in the clinic, a phase I clinical trial of ISB 1342 in r/rMM patients is ongoing (NCT03309111)(69).

Acknowledgements

We thank Camille Grandclément, Evangelia Martini, Valentina Labanca, Stefania De Angelis, Isabelle Gruber, Jérémy Berret, Elodie Stainnack, Riccardo Turrini, Estelle Gerossier, Alain Rubod, Min Ma, Tania Melly, Debora Lind, Paul Oster, Estelle Etasse and Antoine Job for their technical assistance with the *ex vivo* and *in vivo* models. We thank Viviane Villard for providing ISB 1342 We thanks Sunitha Gn (Glenmark) for her work on the IP-LC/MS/MS method. We thank our past Ichnos Sciences SA members Christelle Ries-Fecourt, Cian Stutz, Amélie Croset, Mégane Pluess, Romain Ollier, Darko Skegro for their help with developing ISB 1342. We thank Cyrille Touzeau, Nicoletta Lilli and Sophie Maïga for access to the patient samples from the MYRACLE (Myeloma Resistance And Clonal Evolution) cohort at CHU Nantes (France). We thank Cindy Lanvers for her help in collecting patient samples at University Hospital Geneva (Switzerland). We are grateful to Dr. Sarah Gooding and Mirian Salazar, all patients who donated samples and the HaemBio Biobank, a Medical Research Council and Oxford Biomedical Research Centre (BRC) funded Biobank, at the MRC Molecular Haematology Unit, Weatherall Institute of Molecular Medicine, University of Oxford, Headley Way, Oxford, OX3 SDS, for the provision of clinical samples. We thank Jairo A. Matthews and Steven M. Kornblau at the UT MD Anderson Cancer Center, Department of Leukemia, Leukemia Sample Bank for access to T-ALL patient samples.

Authorship Contributions

B.P, C.E, P.S, E.N, A.L, T.M, A.C, D.P, L.C, J.M, J. B and M.C contributed to assay design, data acquisition, interpretation and analysis. Z.K, E.M, C.K, contributed to acquisition of data, and analysis, interpretation of patient samples experiments. T.M, C.P-D, P.M, C.M.E, J.R.E, A.M, G.B contributed to the acquisition of patient samples and discussion of data interpretation. G.G, V.U and V.M supervised, analysed and interpreted the cynomolgus

monkey studies. B.P, M.L.M, A.D, M.Pi, M-A.D, A.S, S.B, E.Z, M.P, M.C contributed to project and resources administration, resources and supervision. B.P, P.S, C.E, A.D, S.B, A.S, M.Pi, MA.D, E.Z, reviewed and edited the manuscript. B.P, C.E, M.P and M.C wrote, reviewed and edited the manuscript.

Conflict of interest Statement

B. Pouleau, C. Estoppey, P. Suere, E. Nallet A. Laurendon, T. Monney, D. Pais, A. Drake, L. Carretero, J. Macoin, M. Pihlgren, M. A. Doucey, G. Gudi, V. Menon, A. Srivastava, E. Zhukovsky, M. Perro and M. Chimen are employees of Ichnos Sciences.

All remaining authors declare no competing interests.

ORCID profiles:

Myriam Chimen: 0000-0002-3567-1731; Mario Perro: 0000-0003-1375-8155; Thomas Matthes: 0000-0002-4875-2477; Catherine Pellat-Deceunynck 0000-0002-6287-8148.

References

1. Sung H, Ferlay J, Siegel RL, Laversanne M, Soerjomataram I, Jemal A, et al. Global Cancer Statistics 2020: GLOBOCAN Estimates of Incidence and Mortality Worldwide for 36 Cancers in 185 Countries. CA Cancer J Clin. 2021 May;71(3):209–49.

2. Usmani S, Ahmadi T, Ng Y, Lam A, Desai A, Potluri R, et al. Analysis of Real-World Data on Overall Survival in Multiple Myeloma Patients With ≥3 Prior Lines of Therapy Including a Proteasome Inhibitor (PI) and an Immunomodulatory Drug (IMiD), or Double Refractory to a PI and an IMiD. The Oncologist. 2016 Nov 1;21(11):1355–61.

3. Usmani SZ, Weiss BM, Plesner T, Bahlis NJ, Belch A, Lonial S, et al. Clinical efficacy of daratumumab monotherapy in patients with heavily pretreated relapsed or refractory multiple myeloma. Blood. 2016 Jul 7;128(1):37–44.

4. van de Donk NWCJ, Usmani SZ. CD38 Antibodies in Multiple Myeloma: Mechanisms of Action and Modes of Resistance. Front Immunol. 2018 Sep 20;9:2134.

5. Overdijk MB, Jansen JHM, Nederend M, Lammerts van Bueren JJ, Groen RWJ, Parren PWHI, et al. The Therapeutic CD38 Monoclonal Antibody Daratumumab Induces Programmed Cell Death via Fcγ Receptor–Mediated Cross-Linking. J Immunol. 2016 Aug 1;197(3):807–13.

6. Bapatla A, Kaul A, Dhalla PS, Armenta-Quiroga AS, Khalid R, Garcia J, et al. Role of Daratumumab in Combination With Standard Therapies in Patients With Relapsed and Refractory Multiple Myeloma. Cureus [Internet]. 2021 Jun 4 [cited 2022 Mar 23]; Available from: https://www.cureus.com/articles/59700-role-of-daratumumab-in-combination-with-standard-therapies-in-patients-with-relapsed-and-refractory-multiple-myeloma

7. Palumbo A, Chanan-Khan A, Weisel K, Nooka AK, Masszi T, Beksac M, et al. Daratumumab, Bortezomib, and Dexamethasone for Multiple Myeloma. N Engl J Med. 2016 Aug 25;375(8):754–66.

8. Dimopoulos MA, Oriol A, Nahi H, San-Miguel J, Bahlis NJ, Usmani SZ, et al. Daratumumab, Lenalidomide, and Dexamethasone for Multiple Myeloma. N Engl J Med. 2016 Oct 6;375(14):1319–31.

9. Krejcik J, Frerichs KA, Nijhof IS, van Kessel B, van Velzen JF, Bloem AC, et al. Monocytes and Granulocytes Reduce CD38 Expression Levels on Myeloma Cells in Patients Treated with Daratumumab. Clin Cancer Res. 2017 Dec 15;23(24):7498–511.

10. Saltarella I, Desantis V, Melaccio A, Solimando AG, Lamanuzzi A, Ria R, et al. Mechanisms of Resistance to Anti-CD38 Daratumumab in Multiple Myeloma. Cells. 2020 Jan 9;9(1):167.

11. Nijhof IS, Casneuf T, van Velzen J, van Kessel B, Axel AE, Syed K, et al. CD38 expression and complement inhibitors affect response and resistance to daratumumab therapy in myeloma. Blood. 2016 Aug 18;128(7):959–70.

12. Cho SF, Yeh TJ, Anderson KC, Tai YT. Bispecific antibodies in multiple myeloma treatment: A journey in progress. Front Oncol. 2022 Oct 18;12:1032775.

13. Skegro D, Stutz C, Ollier R, Svensson E, Wassmann P, Bourquin F, et al. Immunoglobulin domain interface exchange as a platform technology for the generation of Fc heterodimers and bispecific antibodies. J Biol Chem. 2017 Jul;292(23):9745–59.

14. Stutz C, Blein S. A single mutation increases heavy-chain heterodimer assembly of bispecific antibodies by inducing structural disorder in one homodimer species. J Biol Chem. 2020 Jul;295(28):9392–408.

15. Carter P. Improving the efficacy of antibody-based cancer therapies. Nat Rev Cancer. 2001 Nov;1(2):118–29.

16. Müller D, Kontermann RE. Recombinant bispecific antibodies for cellular cancer immunotherapy. Curr Opin Mol Ther. 2007 Aug;9(4):319–26.

17. Benaniba L, Tessoulin B, Trudel S, Pellat-Deceunynck C, Amiot M, Minvielle S, et al. The MYRACLE protocol study: a multicentric observational prospective cohort study of patients with multiple myeloma. BMC Cancer. 2019 Dec;19(1):855.

18. Mancardi D, Daëron M. Fc Receptors in Immune Responses. In: Reference Module in Biomedical Sciences [Internet]. Elsevier; 2014 [cited 2022 Nov 8]. p. B9780128012383000000. Available from: https://linkinghub.elsevier.com/retrieve/pii/B9780128012383001197

19. Sewnath CAN, Behrens LM, van Egmond M. Targeting myeloid cells with bispecific antibodies as novel immunotherapies of cancer. Expert Opin Biol Ther. 2022 Aug 3;22(8):983–95.

20. Hezareh M, Hessell AJ, Jensen RC, van de Winkel JGJ, Parren PWHI. Effector Function Activities of a Panel of Mutants of a Broadly Neutralizing Antibody against Human Immunodeficiency Virus Type 1. J Virol. 2001 Dec 15;75(24):12161–8.

21. Wines BD, Powell MS, Parren PWHI, Barnes N, Hogarth PM. The IgG Fc Contains Distinct Fc Receptor (FcR) Binding Sites: The Leukocyte Receptors FcγRI and FcγRIIa Bind to a Region in the Fc Distinct from That Recognized by Neonatal FcR and Protein A. J Immunol. 2000 May 15;164(10):5313–8.

22. Trinklein ND, Pham D, Schellenberger U, Buelow B, Boudreau A, Choudhry P, et al. Efficient tumor killing and minimal cytokine release with novel T-cell agonist bispecific antibodies. mAbs. 2019 May 19;11(4):639–52.

23. Zuch de Zafra CL, Fajardo F, Zhong W, Bernett MJ, Muchhal US, Moore GL, et al. Targeting Multiple Myeloma with AMG 424, a Novel Anti-CD38/CD3 Bispecific T-cell–recruiting Antibody Optimized for Cytotoxicity and Cytokine Release. Clin Cancer Res. 2019 Jul 1;25(13):3921–33.

24. Hogan KA, Chini CCS, Chini EN. The Multi-faceted Ecto-enzyme CD38: Roles in Immunomodulation, Cancer, Aging, and Metabolic Diseases. Front Immunol. 2019 May 31;10:1187.

25. Tvedt THA, Vo AK, Bruserud Ø, Reikvam H. Cytokine Release Syndrome in the Immunotherapy of Hematological Malignancies: The Biology behind and Possible Clinical Consequences. J Clin Med. 2021 Nov 6;10(21):5190.

26. Yang Y, Lundqvist A. Immunomodulatory Effects of IL-2 and IL-15; Implications for Cancer Immunotherapy. Cancers. 2020 Nov 30;12(12):3586.

27. Cremasco F, Menietti E, Speziale D, Sam J, Sammicheli S, Richard M, et al. Cross-linking of T cell to B cell lymphoma by the T cell bispecific antibody CD20-TCB induces IFNγ/CXCL10-dependent peripheral T cell recruitment in humanized murine model. Najbauer J, editor. PLOS ONE. 2021 Jan 6;16(1):e0241091.

28. Li J, Ybarra R, Mak J, Herault A, De Almeida P, Arrazate A, et al. IFNγ-induced Chemokines Are Required for CXCR3-mediated T-Cell Recruitment and Antitumor Efficacy of Anti-HER2/CD3 Bispecific Antibody. Clin Cancer Res. 2018 Dec 15;24(24):6447–58.

29. Codarri Deak L, Nicolini V, Hashimoto M, Karagianni M, Schwalie PC, Lauener L, et al. PD-1-cis IL-2R agonism yields better effectors from stem-like CD8+ T cells. Nature. 2022 Oct 6;610(7930):161–72.

30. Tichet M, Wullschleger S, Chryplewicz A, Fournier N, Marcone R, Kauzlaric A, et al. Bispecific PD1-IL2v and anti-PD-L1 break tumor immunity resistance by enhancing stem-like tumor-reactive CD8+ T cells and reprogramming macrophages. Immunity. 2023 Jan;56(1):162-179.e6.

31. Morris EC, Neelapu SS, Giavridis T, Sadelain M. Cytokine release syndrome and associated neurotoxicity in cancer immunotherapy. Nat Rev Immunol. 2022 Feb;22(2):85–96.

32. Römer PS, Berr S, Avota E, Na SY, Battaglia M, ten Berge I, et al. Preculture of PBMCs at high cell density increases sensitivity of T-cell responses, revealing cytokine release by CD28 superagonist TGN1412. Blood. 2011 Dec 22;118(26):6772–82.

33. Saber H, Del Valle P, Ricks TK, Leighton JK. An FDA oncology analysis of CD3 bispecific constructs and first-in-human dose selection. Regul Toxicol Pharmacol. 2017 Nov;90:144–52.

34. van de Donk NWCJ, Richardson PG, Malavasi F. CD38 antibodies in multiple myeloma: back to the future. Blood. 2018 Jan 4;131(1):13–29.

35. Morandi F, Horenstein AL, Costa F, Giuliani N, Pistoia V, Malavasi F. CD38: A Target for Immunotherapeutic Approaches in Multiple Myeloma. Front Immunol. 2018 Nov 28;9:2722.

36. Offidani M, Corvatta L, Morè S, Nappi D, Martinelli G, Olivieri A, et al. Daratumumab for the Management of Newly Diagnosed and Relapsed/Refractory Multiple Myeloma: Current and Emerging Treatments. Front Oncol. 2021 Feb 17;10:624661.

37. Lonial S, Weiss BM, Usmani SZ, Singhal S, Chari A, Bahlis NJ, et al. Daratumumab monotherapy in patients with treatment-refractory multiple myeloma (SIRIUS): an open-label, randomised, phase 2 trial. The Lancet. 2016 Apr;387(10027):1551–60.

38. Mateos MV, Dimopoulos MA, Cavo M, Suzuki K, Jakubowiak A, Knop S, et al. Daratumumab plus Bortezomib, Melphalan, and Prednisone for Untreated Myeloma. N Engl J Med. 2018 Feb 8;378(6):518–28.

39. Gandhi UH, Cornell RF, Lakshman A, Gahvari ZJ, McGehee E, Jagosky MH, et al. Outcomes of patients with multiple myeloma refractory to CD38-targeted monoclonal antibody therapy. Leukemia. 2019 Sep;33(9):2266–75.

40. Shen F, Shen W. Isatuximab in the Treatment of Multiple Myeloma: A Review and Comparison With Daratumumab. Technol Cancer Res Treat. 2022 Jan;21:153303382211065.

41. Doucey MA, Pouleau B, Estoppey C, Stutz C, Croset A, Laurendon A, et al. ISB 1342: A first-in-class CD38 T cell engager for the treatment of relapsed refractory multiple myeloma. J Clin Oncol. 2021 May 20;39(15_suppl):8044–8044.

42. Wu L, Seung E, Xu L, Rao E, Lord DM, Wei RR, et al. Trispecific antibodies enhance the therapeutic efficacy of tumor-directed T cells through T cell receptor co-stimulation. Nat Cancer. 2020 Jan;1(1):86–98.

43. Maxime Fayon, Carolina Martinez-Cingolani, Audrey Abecassis, Nathalie Roders, Elisabeth Nelson, Caroline Choisy, et al. Bi38-3 is a novel CD38/CD3 bispecific T-cell engager with low toxicity for the treatment of multiple myeloma. Haematologica. 2020 Jul 16;106(4):1193–7.

44. Plesner T, van de Donk NWCJ, Richardson PG. Controversy in the Use of CD38 Antibody for Treatment of Myeloma: Is High CD38 Expression Good or Bad? Cells. 2020 Feb 6;9(2):378.

45. van de Donk NWCJ, Usmani SZ. CD38 Antibodies in Multiple Myeloma: Mechanisms of Action and Modes of Resistance. Front Immunol. 2018 Sep 20;9:2134.

46. Nijhof IS, Groen RWJ, Lokhorst HM, van Kessel B, Bloem AC, van Velzen J, et al. Upregulation of CD38 expression on multiple myeloma cells by all-trans retinoic acid improves the efficacy of daratumumab. Leukemia. 2015 Oct;29(10):2039–49.

47. Pilcher W, Thomas BE, Bhasin SS, Jayasinghe RG, Rahman AH, Kim-Schulze S, et al. Characterization of T-Cell Exhaustion in Rapid Progressing Multiple Myeloma Using Cross Center Scrna-Seq Study. Blood. 2021 Nov 5;138(Supplement 1):401–401.

48. Chung DJ, Pronschinske KB, Shyer JA, Sharma S, Leung S, Curran SA, et al. T-cell Exhaustion in Multiple Myeloma Relapse after Autotransplant: Optimal Timing of Immunotherapy. Cancer Immunol Res. 2016 Jan 1;4(1):61–71.

49. Philipp N, Kazerani M, Nicholls A, Vick B, Wulf J, Straub T, et al. T-cell exhaustion induced by continuous bispecific molecule exposure is ameliorated by treatment-free intervals. Blood. 2022 Sep 8;140(10):1104–18.

50. Pillarisetti K, Powers G, Luistro L, Babich A, Baldwin E, Li Y, et al. Teclistamab is an active T cell–redirecting bispecific antibody against B-cell maturation antigen for multiple myeloma. Blood Adv. 2020 Sep 22;4(18):4538–49.

51. Verkleij CPM, Broekmans MEC, van Duin M, Frerichs KA, Kuiper R, de Jonge AV, et al. Preclinical activity and determinants of response of the GPRC5DxCD3 bispecific antibody talquetamab in multiple myeloma. Blood Adv. 2021 Apr 27;5(8):2196–215.

52. Sam J, Colombetti S, Fauti T, Roller A, Biehl M, Fahrni L, et al. Combination of T-Cell Bispecific Antibodies With PD-L1 Checkpoint Inhibition Elicits Superior Anti-Tumor Activity. Front Oncol. 2020 Nov 30;10:575737.

53. Stoltzfus CR, Sivakumar R, Kunz L, Olin Pope BE, Menietti E, Speziale D, et al. Multi-Parameter Quantitative Imaging of Tumor Microenvironments Reveals Perivascular Immune Niches Associated With Anti-Tumor Immunity. Front Immunol. 2021 Aug 5;12:726492.

54. Mouhieddine TH, Van Oekelen O, Melnekoff DT, Li J, Ghodke-Puranik Y, Lancman G, et al. Sequencing T-cell redirection therapies leads to deep and durable responses in relapsed/refractory myeloma patients. Blood Adv. 2022 Aug 26;bloodadvances.2022007923.

55. Samur MK, Fulciniti M, Aktas Samur A, Bazarbachi AH, Tai YT, Prabhala R, et al. Biallelic loss of BCMA as a resistance mechanism to CAR T cell therapy in a patient with multiple myeloma. Nat Commun. 2021 Feb 8;12(1):868.

56. Da Vià MC, Dietrich O, Truger M, Arampatzi P, Duell J, Heidemeier A, et al. Homozygous BCMA gene deletion in response to anti-BCMA CAR T cells in a patient with multiple myeloma. Nat Med. 2021 Apr;27(4):616–9.

57. Chen H, Li M, Xu N, Ng N, Sanchez E, Soof CM, et al. Serum B-cell maturation antigen (BCMA) reduces binding of anti-BCMA antibody to multiple myeloma cells. Leuk Res. 2019 Jun;81:62–6.

58. Lee H, Maity R, Ahn S, Leblay N, Tilmont R, Barakat E, et al. OAB-005: Point mutations in BCMA extracellular domain mediate resistance to BCMA targeting immune therapies. Clin Lymphoma Myeloma Leuk. 2022 Aug;22:S3–4.

59. Green DJ, Pont M, Cowan AJ, Cole GO, Sather BD, Nagengast AM, et al. Response to Bcma CAR-T Cells Correlates with Pretreatment Target Antigen Density and Is Improved By Small Molecule Inhibition of Gamma Secretase. Blood. 2019 Nov 13;134(Supplement_1):1856–1856.

60. Obstfeld AE, Frey NV, Mansfield K, Lacey SF, June CH, Porter DL, et al. Cytokine release syndrome associated with chimeric-antigen receptor T-cell therapy: clinicopathological insights. Blood. 2017 Dec 7;130(23):2569–72.

61. Lee DW, Santomasso BD, Locke FL, Ghobadi A, Turtle CJ, Brudno JN, et al. ASTCT Consensus Grading for Cytokine Release Syndrome and Neurologic Toxicity Associated with Immune Effector Cells. Biol Blood Marrow Transplant. 2019 Apr;25(4):625–38.

62. Karki R, Kanneganti TD. The 'cytokine storm': molecular mechanisms and therapeutic prospects. Trends Immunol. 2021 Aug;42(8):681–705.

63. Shimabukuro-Vornhagen A, Gödel P, Subklewe M, Stemmler HJ, Schlößer HA, Schlaak M, et al. Cytokine release syndrome. J Immunother Cancer. 2018 Dec;6(1):56.

64. Lee DW, Gardner R, Porter DL, Louis CU, Ahmed N, Jensen M, et al. Current concepts in the diagnosis and management of cytokine release syndrome. Blood. 2014 Jul 10;124(2):188–95.

65. Usmani SZ, Garfall AL, van de Donk NWCJ, Nahi H, San-Miguel JF, Oriol A, et al. Teclistamab, a B-cell maturation antigen × CD3 bispecific antibody, in patients with relapsed or refractory multiple myeloma (MajesTEC-1): a multicentre, open-label, single-arm, phase 1 study. The Lancet. 2021 Aug;398(10301):665–74.

66. Bacac M, Colombetti S, Herter S, Sam J, Perro M, Chen S, et al. CD20-TCB with Obinutuzumab Pretreatment as Next-Generation Treatment of Hematologic Malignancies. Clin Cancer Res. 2018 Oct 1;24(19):4785–97.

67. Carlo-Stella C, Khan C, Hutchings M, Offner FC, Morschhauser F, Bachy E, et al. ABCL-360: Glofitamab Step-Up Dosing (SUD): Updated Efficacy Data Show High Complete Response Rates in Heavily Pretreated Relapsed/Refractory (R/R) Non-Hodgkin Lymphoma (NHL) Patients (Pts). Clin Lymphoma Myeloma Leuk. 2021 Sep;21:S394.

68. Leclercq G, Steinhoff N, Haegel H, De Marco D, Bacac M, Klein C. Novel strategies for the mitigation of cytokine release syndrome induced by T cell engaging therapies with a focus on the use of kinase inhibitors. OncoImmunology. 2022 Dec 31;11(1):2083479.

69. Mohan SR, Costa Chase C, Berdeja JG, Karlin L, Belhadj K, Perrot A, et al. Initial Results of Dose Escalation of ISB 1342, a Novel CD3xCD38 Bispecific Antibody, in Patients with Relapsed / Refractory Multiple Myeloma (RRMM). Blood. 2022 Nov 15;140(Supplement 1):7264–6.

Tables

Table 1: Summary PK Parameters of ISB 1342 in Cynomolgus Monkeys: consecutive doses study

Dose level (µg/kg)	C_0 (ng/mL)	C_{max} (ng/mL)	T_{max} (hr)	AUC_{0-t} (hr*ng/mL)	t_{last} (hr)	$AUC_{0-\infty}$ (hr*ng/mL)	$t_{1/2}$ (hr)	ADA detected
1	NE	0.44	4.0	8.8	36	NE	NE	None
100	206	131	4.0	4589	252	4863	58.2[a]	Day 43
1000	462	165.95	4.0	2193	16	4355[a]	2.8	Day 43

[a] N=1

$AUC_{0-\infty}$ = area under the (serum) concentration time curve extrapolated out to infinity; AUC_{0-t} = area under the plasma concentration-time curve from time zero to time t; C_0 = initial concentration; NE: Not Estimable; $t_{½}$= terminal elimination half-life; t_{last} = time of the last measurable (positive) concentration; T_{max}= Time to reach maximum serum concentration following drug administration. ADA = Anti-Drug Antibodies.

Figure Legends

Figure 1. ISB 1342 properties and binding. (A) Schematic 3D representation of ISB 1342, a bispecific antibody based on the BEAT® technology with a Fab targeting CD38, an scFv targeting CD3ε and Fc carrying the LALA (L234A, L235A) mutation. The model was generated using the BioLuminate software (Schrödinger, USA). (B) Mean ± SD of K_D determined either on $CD38^-$ T-cells (n=12 donors in 3 independent experiments) and MM cells lines, KMS-12-BM (20 measures from n=14 idependent experiments), NCI-H929 (12 measures from n=5 idependent experiments) and MOLP-8 (9 measures from n=3 idependent experiments), or recombinant human proteins CD3εδ (n=5 independent experiments) and CD38 (n=3 independent experiments) (C) Representative binding of ISB 1342 on $CD38^-$ human healthy T-cells (mean ± SD of 4 donors) and KMS-12-BM MM cell line (one representative measurement from one experiment). (D) Epitope mapping of daratumumab and ISB 1342 on CD38. Residues in dark red represent the CD38 residues in a 4 Å radius from the daratumumab

chain in the crystal structure 7DHA. Linear peptides mapping by SPR as well as site-directed mutagenesis were used to determine the binding epitope of ISB 1342 on CD38, shown in green on the CD38 chain of crystal structure 7DHA (in beige color). (E) ISB 1342 does not compete with daratumumab and can engage CD38 prebound by daratumumab. Biotinylated human CD38 protein was loaded on a streptavidin SA Biosensor. Biosensor with immobilized CD38 was then dipped in a solution of daratumumab in kinetics buffer to reach saturation of the surface. Then, saturated biosensor was dipped into a pre-mixed solution of daratumumab + ISB 1342 at equimolar concentrations (pink curve) or daratumumab only (black curve). Plots show binding to the sensor tip as a wavelength shift (Response, in nm; Y axis) vs. time (in sec; X axis).

Figure 2: ISB1342 induces killing of MM cell lines *in vitro* via T-cell engagement. (A) Representative confocal image of ISB 1342 (white) at the synapse between T-cell (green) and KMS-12-BM MM cell line (blue) acquired with Zeiss LSM 800 inverted confocal microscope, magnification 40X. (B-F) Cytotoxicity of KMS-12-BM MM cell line (B, F) and T-cell activation (C), proliferation (D) and degranulation (E) after treatment with ISB 1342 or control molecules in presence (F) or absence (B-E) of soluble CD38 (sCD38) and healthy PBMC (E:T 5:1) for 72 hours. Data represent mean ± SD from 3 PBMC donors performed in 2 independent experiments (B-E) or mean ± SD of EC_{50} from 3 donors that were compared to the condition without sCD38 using a one-way ANOVA followed by a Dunnett's post-hoc comparison (F), ns: not significant. (G-H) Cytotoxicity of RPMI8226 MM cell line (G) and cytokine release (H) in presence of ISB 1342 ± Dexamethasone and healthy PBMC (E:T 10:1) for 48 hours. Data represent mean ± SD of EC_{50} compared using a paired t-test (G) and mean ± SD at the maximum dose of ISB 1342 tested compared using paired t-test (H) from 6 PBMC donors and performed in 2 independent experiments; ** $p<0.01$, *** $p<0.001$.

Figure 3: ISB 1342 induces potent killing of cell lines showing a reduced sensitivity to daratumumab. (A) Absolute number of specific Antibody Bound per Cell (sABC) indicating the relative CD38 density on MM cell lines. Data represent mean ± SD and compared using a one-way ANOVA followed by a Kruskall-Wallis post-hoc comparison using KMS-12-BM as reference. (B-D) Cytotoxicity of MM cell lines in presence of daratumumab in CDC (B), ADCP (C) and ADCC (D) assays. Data represent mean ± SD of maximum response from 4 donors in 2 independent experiments (B), from up to 10 donors in 3 independent experiments (C) and from 5 donors in 3 independent experiments (D) that were compared using a one-way ANOVA followed by a Tukey post-hoc comparison. (E) Cytotoxicity of MM cell lines in presence of ISB 1342 and healthy PBMC (E:T 5:1) for 72 hours in a RDL assay. Data represent mean ± SD of EC_{50} from 6 PBMC donors, compared using a one-way ANOVA followed by Dunnett's post-hoc comparison to KMS-12-BM. (F-H) Schematic representation depicting the Multiple Mode of Action (MoA) Killing in vitro assay (MMoAK) including four MoA: T-cell RDL, ADCC, ADCP and CDC (F). Cytotoxicity of various MM cell lines in presence of ISB 1342 or daratumumab, healthy PBMC (E:T 5:1), normal human serum and rhIL-2 for 48 hours in a MMoAK assay. Data represent mean ± SD of duplicates from one representative donor using non-linear regression analysis (F), mean ± SD of EC_{50} from up to 10 PBMC donors per treatment and cell line from 6 independent experiments that were compared using a two-way ANOVA and Sidak's post-test (G-H); *$p<0.05$, **$p<0.01$, ***$p<0.0001$, ****$p<0.00001$.

Figure 4: ISB 1342 *in vitro* potency is not impacted by the concomitant or pre-treatment with daratumumab. (A) Schematic representation depicting the MMoAK assay with concomitant treatment with ISB 1342 and daratumumab. (B, C) Cytotoxicity of NCI-H929 MM cell line (B) and $CD8^+$ T-cell response (C) following treatment with increasing doses of ISB 1342 and a fixed dose daratumumab or monoclonal antibody control (mAb) in presence of healthy PBMC (E:T 5:1), normal human serum and rhIL-2 for 48 hours. Data represent mean ± SD of EC_{50} or the maximum response from 12 donors in 3 independent experiments that were compared using an unpaired T-test. (D) Schematic representation depicting the MMoAK assay of pre-treatment with daratumumab followed by ISB 1342. (E,F) Cytotoxicity of NCI-H929 MM cell line (E) and $CD8^+$ T-cell response (F) in presence of healthy PBMC (E:T 5:1),

normal human serum and rhIL-2 with increasing doses of ISB 1342 for 48 hours after pre-treatment with a fix dose daratumumab or monoclonal antibody control for 24h. Data represent mean ± SD of EC_{50} or the maximum response from up to 9 donors in 3 independent experiments that were compared using an unpaired T-test; ns: not significant.

Figure 5: ISB 1342 maintains high potency to kill tumour cells from patients previously treated with daratumumab. (A-C) Representative cytotoxicity curves of $CD138^+$ MM cells by ISB 1342 and daratumumab at 18-24h in samples from patients not previously treated with daratumumab (dara-naïve, patient sample 4) (A), previously treated with daratumumab (dara-exposed, patient sample 15) (B) and dara-naïve plasma cell leukemia (PCL, patient sample 1) (C). Data are mean (A, B) or mean ± SEM of replicates (C) analysed using non-linear regression analysis. (D) Maximal cytotoxicity of $CD138^+$ tumor cells with ISB 1342 (10-100nM) or daratumumab (100nM) in samples from dara-naïve patients (filled symbols) versus dara-exposed (open symbols). Dots represent individual samples and data are mean ± SD compared using one-way ANOVA followed by Dunnett's multiple comparison analysis to daratumumab on dara-naive samples. (E) Radar plot of average values for $CD8^+$T-cells, NK cells and Monocytes/Macrophages ratio to $CD138^+$ MM cells in samples from dara-naïve patients (blue) versus dara-exposed ones (pink). (F) Representative $CD8^+$ T-cell activation with ISB 1342 and isotype control measured by flow cytometry with expression of CD69 (blue) and CD25 (pink) in PCL. Data are mean ± SEM of replicates analysed using non-linear regression analysis. (G) Maximum T-cell activation (CD25 and CD69) and degranulation (CD107a) on dara-naïve versus dara-exposed patient samples with ISB 1342. Data are mean ± SD compared using unpaired t-test.

Figure 6: ISB 1342 controlled tumor growth *in vivo* in the KMS-12-BM xenograft hPBMC-transferred NSG mouse model. (A-B) Experimental design (A) and measurement of tumor growth (B) in the KMS-12-BM s.c. xenograft human PBMC (hPBMC)-transferred NSG mouse model. *In vivo* activity was followed for ISB 1342 at 0.5 mg/Kg injected i.v. once per week and daratumumab at 16 mg/Kg injected i.v. twice per week, both for three weeks with 8 mice per group. Data are mean mm^3 ± SD determined by caliper measurements. Data were compared for both models using two-way ANOVA followed by Tukey's post-hoc comparison. * is showing significant differences between ISB 1342 and vehicle control; # is showing differences between daratumumab and ISB 1342. (C-D) Infiltration of hCD45+ cells (defined as live $hCD45^+mCD45^-$) (C) and T-cells ($hTCR\alpha\beta^+CD14^-CD19^-CD56^-CD45^+$) (D) in tumors of KMS-12-BM xenografted mice after vehicle, ISB1342 or daratumumab treatments. Data are mean ± SD for 5 mice compared using one-way ANOVA followed by Dunnet's post-hoc test to ISB 1342. (E) Representative dot plots showing activation profile (CD25 and CD69 expression) on tumor-infiltrating T-cell activation in vehicle, daratumumab and ISB 1342-treated mice. (F) CD38 expression on MM cells in tumors (KMS-12-BM model). Data are mean ± SD compared using one-way ANOVA followed by Tukey's post-hoc test; *$p \leq 0.05$.

Figure 7: Impact of ISB 1342 on circulating leukocytes and systemic soluble factors in cynomolgus monkeys. (A) Expression profile of CD38 on leukocyte populations from cynomolgus monkeys. Dots represent data the relative fluorescence intensity (RFI) from each measurement and bars represent mean ± SD from 4 animals. Data were compared using a one-way ANOVA followed by Dunnett's post-hoc comparison, *$p \leq 0.05$. (B) Representative binding of ISB 1342 or isotype control on cynomolgus monkey B-cells. (C-H) Cynomolgus monkeys (1 male and 1 female) were injected with 3 consecutives doses of ISB 1342 i.v. (1, 100 and 1000 µg/kg) at day 1, 29 and 57 respectively. Levels of peripheral B-cells (C), monocytes (D), $CD8^+$ T-cells (E), activated $CD8^+$ $CD69^+$ T-cells (F), $CD4^+$ T-cells (G) and activated $CD4^+$ $CD69^+$ T-cells (H) were measured using flow cytometry. Data is mean ± SD of 10^3 counts/µl normalized to baseline counts for two animals. (I,J) Levels of circulating IFN-γ (I) and ISB 1342 (J) were measured using ELISA. Data represent levels per animal and LLOQ is the lower limit of quantification for the assay.

Figure 1

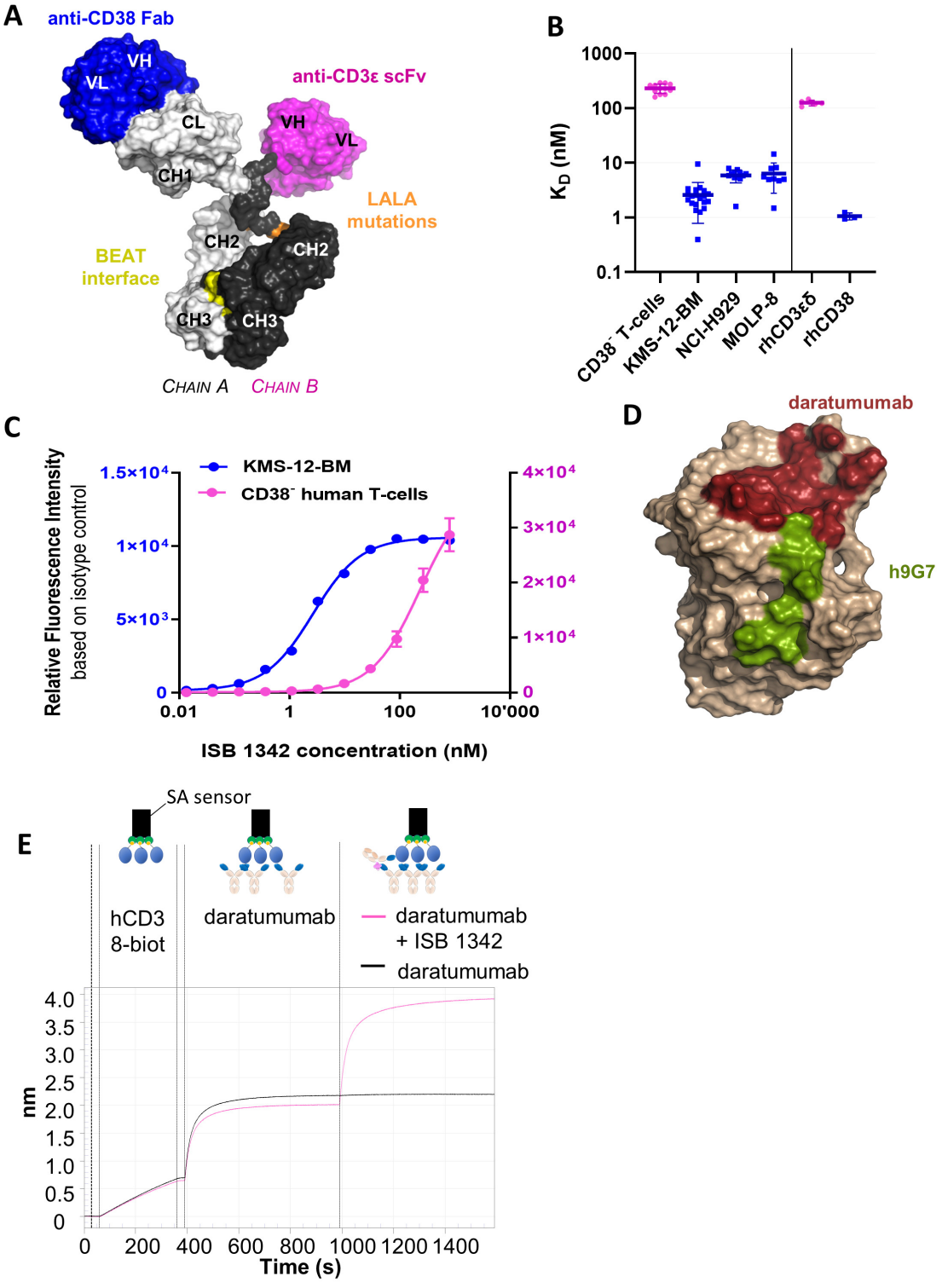
A
anti-CD38 Fab
VH
VL
CL
CH1
anti-CD3ε scFv
VH
VL
LALA
mutations
BEAT
interface
CH2
CH2
CH3
CH3
CHAIN A
CHAIN B
B
1000
100
10
1
0.1
K_D (nM)
CD38⁻ T-cells
KMS-12-BM
NCI-H929
MOLP-8
rhCD3εδ
rhCD38
C
Relative Fluorescence Intensity
based on isotype control
KMS-12-BM
CD38⁻ human T-cells
1.5×10⁴
1×10⁴
5×10³
0
4×10⁴
3×10⁴
2×10⁴
1×10⁴
0
0.01
1
100
10'000
ISB 1342 concentration (nM)
D
daratumumab
h9G7
E
SA sensor
hCD3
8-biot
daratumumab
daratumumab
+ ISB 1342
daratumumab
nm
4.0
3.5
3.0
2.5
2.0
1.5
1.0
0.5
0
0
200
400
600
800
1000
1200
1400
Time (s)

Figure 2

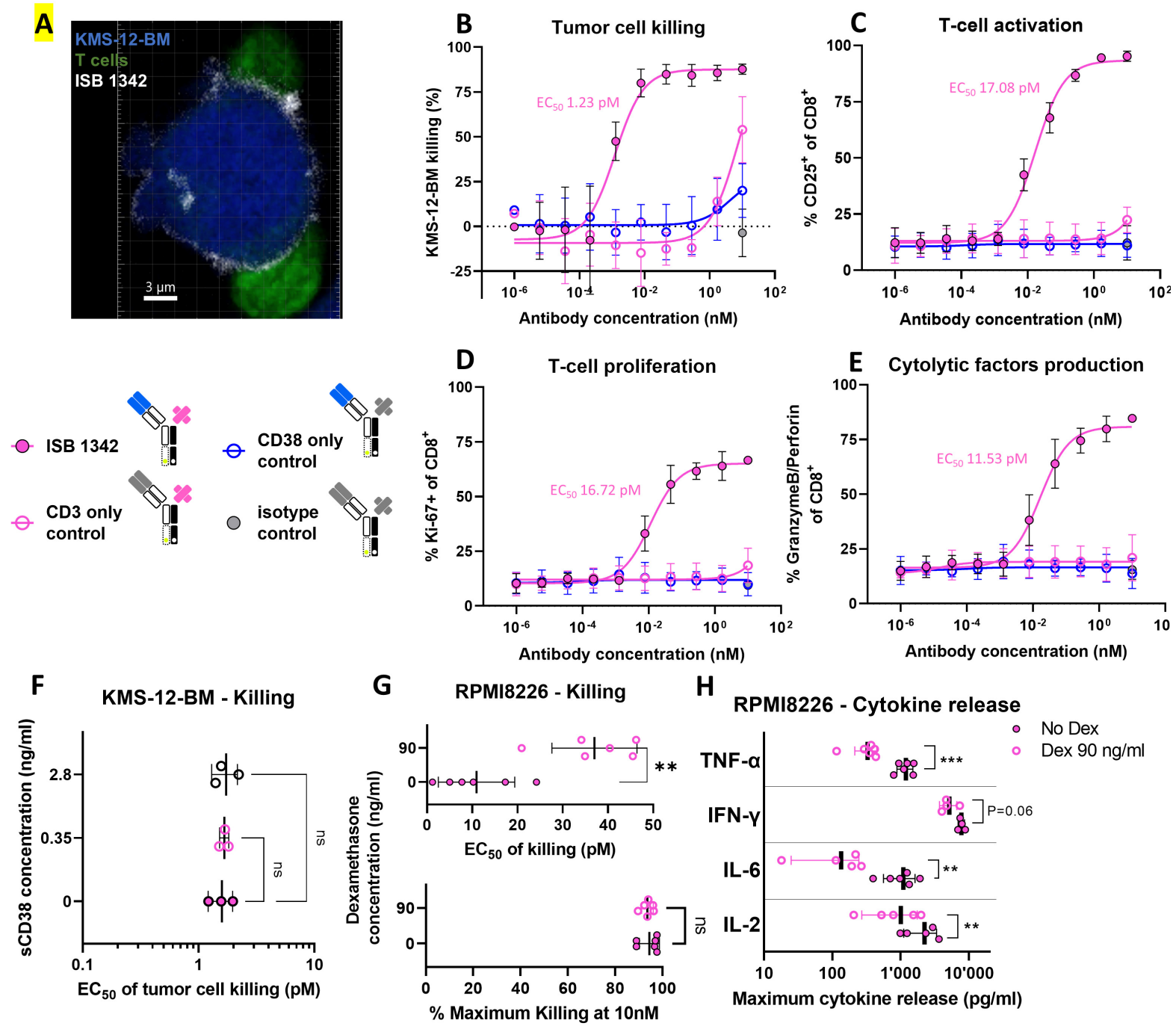
A
KMS-12-BM
T cells
ISB 1342
3 µm
B
Tumor cell killing
KMS-12-BM killing (%)
EC50 1.23 pM
Antibody concentration (nM)
C
T-cell activation
% CD25+ of CD8+
EC50 17.08 pM
Antibody concentration (nM)
ISB 1342
CD3 only control
CD38 only control
isotype control
D
T-cell proliferation
% Ki-67+ of CD8+
EC50 16.72 pM
Antibody concentration (nM)
E
Cytolytic factors production
% GranzymeB/Perforin of CD8+
EC50 11.53 pM
Antibody concentration (nM)
F
KMS-12-BM - Killing
sCD38 concentration (ng/ml)
EC50 of tumor cell killing (pM)
ns
ns
G
RPMI8226 - Killing
Dexamethasone concentration (ng/ml)
EC50 of killing (pM)
**
% Maximum Killing at 10nM
ns
H
RPMI8226 - Cytokine release
No Dex
Dex 90 ng/ml
TNF-α
IFN-γ
IL-6
IL-2
***
P=0.06
**
**
Maximum cytokine release (pg/ml)

Figure 3

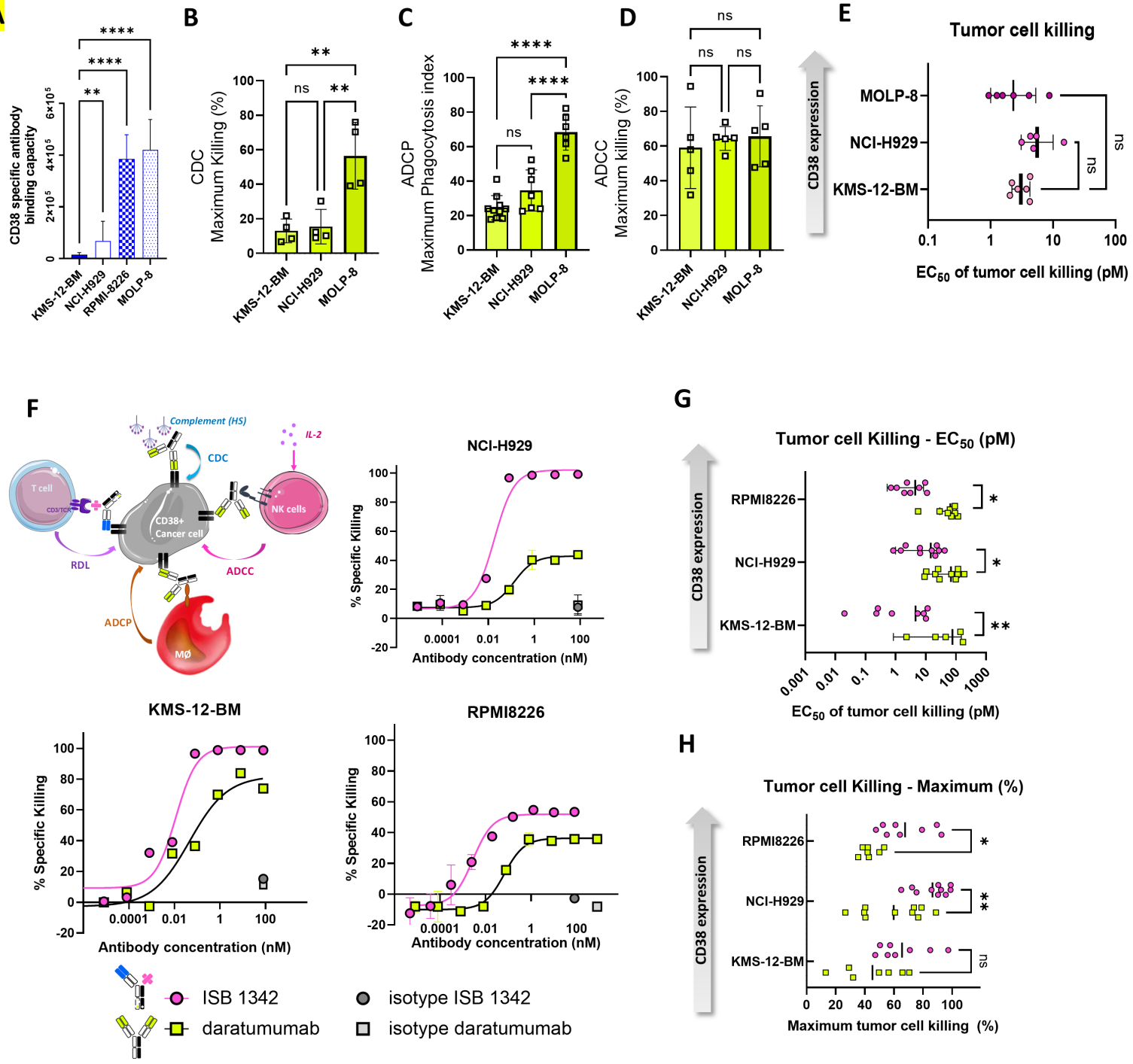
A
CD38 specific antibody binding capacity
KMS-12-BM
NCI-H929
RPMI-8226
MOLP-8
B
CDC
Maximum Killing (%)
C
ADCP
Maximum Phagocytosis index
D
ADCC
Maximum killing (%)
E
Tumor cell killing
CD38 expression
EC50 of tumor cell killing (pM)
F
Complement (HS)
IL-2
CDC
T cell
NK cells
CD38+ Cancer cell
RDL
ADCC
ADCP
MØ
NCI-H929
KMS-12-BM
RPMI8226
% Specific Killing
Antibody concentration (nM)
ISB 1342
daratumumab
isotype ISB 1342
isotype daratumumab
G
Tumor cell Killing - EC50 (pM)
H
Tumor cell Killing - Maximum (%)
Maximum tumor cell killing (%)

Figure 4

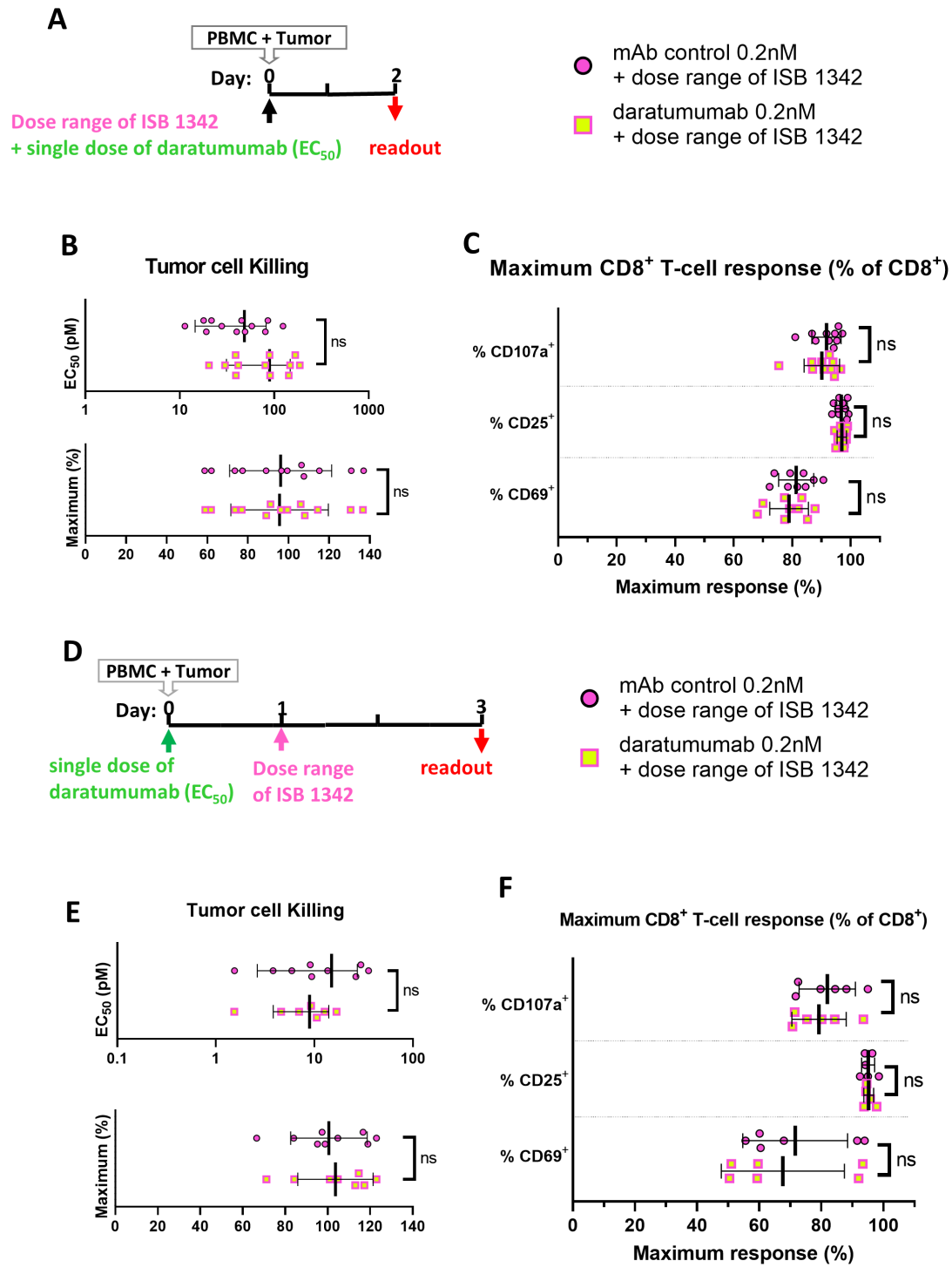
A
PBMC + Tumor
Day: 0
2
Dose range of ISB 1342
+ single dose of daratumumab (EC50)
readout
mAb control 0.2nM
+ dose range of ISB 1342
daratumumab 0.2nM
+ dose range of ISB 1342
B
Tumor cell Killing
EC50 (pM)
ns
1
10
100
1000
Maximum (%)
ns
0
20
40
60
80
100
120
140
C
Maximum CD8+ T-cell response (% of CD8+)
% CD107a+
% CD25+
% CD69+
ns
0
20
40
60
80
100
Maximum response (%)
D
PBMC + Tumor
Day: 0
1
3
single dose of
daratumumab (EC50)
Dose range
of ISB 1342
readout
mAb control 0.2nM
+ dose range of ISB 1342
daratumumab 0.2nM
+ dose range of ISB 1342
E
Tumor cell Killing
EC50 (pM)
ns
0.1
1
10
100
Maximum (%)
ns
0
20
40
60
80
100
120
140
F
Maximum CD8+ T-cell response (% of CD8+)
% CD107a+
% CD25+
% CD69+
ns
0
20
40
60
80
100
Maximum response (%)

Figure 5

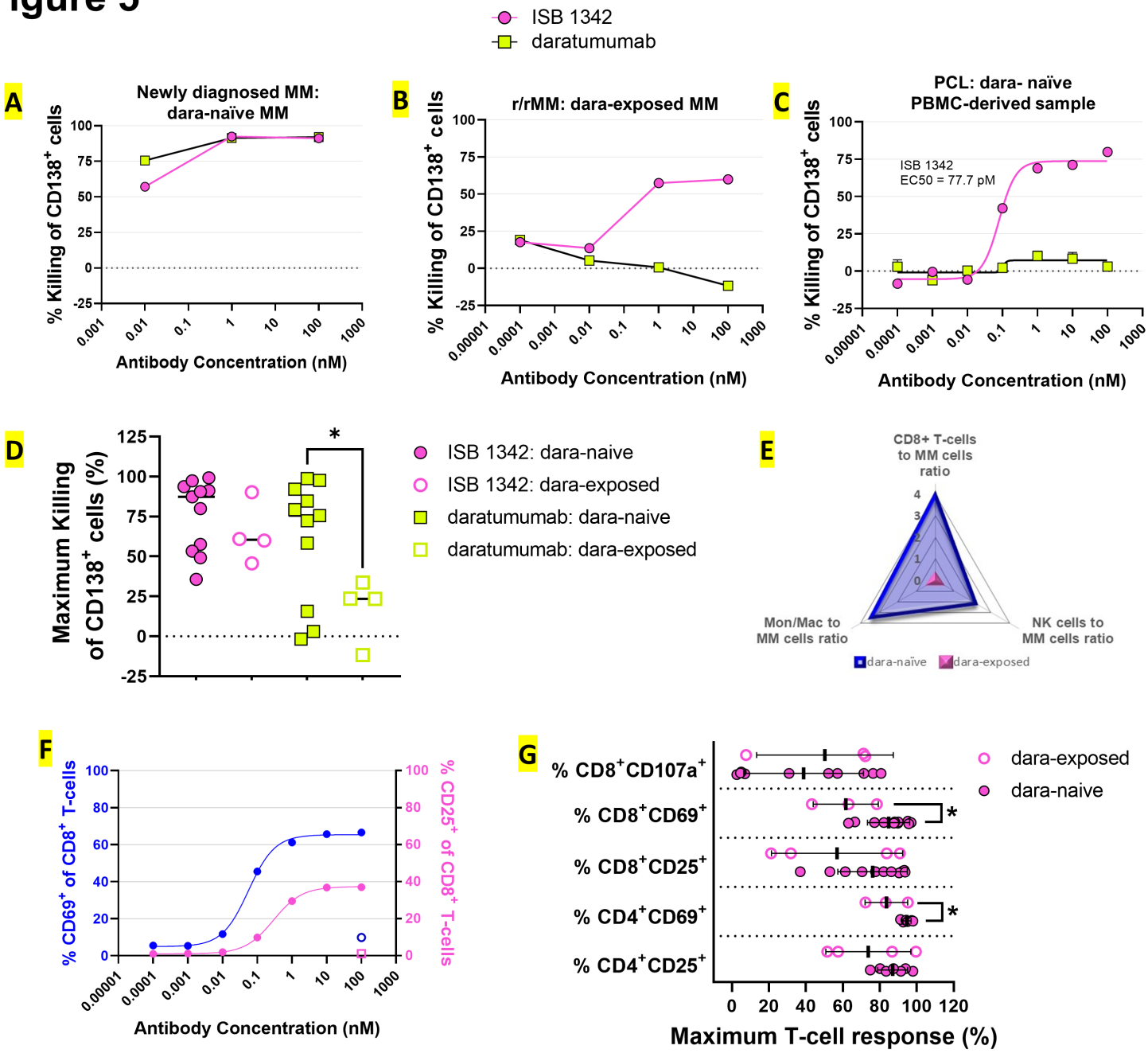
ISB 1342
daratumumab
A
Newly diagnosed MM:
dara-naïve MM
% Killing of CD138+ cells
Antibody Concentration (nM)
B
r/rMM: dara-exposed MM
% Killing of CD138+ cells
Antibody Concentration (nM)
C
PCL: dara- naïve
PBMC-derived sample
ISB 1342
EC50 = 77.7 pM
% Killing of CD138+ cells
Antibody Concentration (nM)
D
Maximum Killing of CD138+ cells (%)
ISB 1342: dara-naive
ISB 1342: dara-exposed
daratumumab: dara-naive
daratumumab: dara-exposed
E
CD8+ T-cells to MM cells ratio
Mon/Mac to MM cells ratio
NK cells to MM cells ratio
dara-naïve
dara-exposed
F
% CD69+ of CD8+ T-cells
% CD25+ of CD8+ T-cells
Antibody Concentration (nM)
G
% CD8+CD107a+
% CD8+CD69+
% CD8+CD25+
% CD4+CD69+
% CD4+CD25+
dara-exposed
dara-naive
Maximum T-cell response (%)

Figure 6

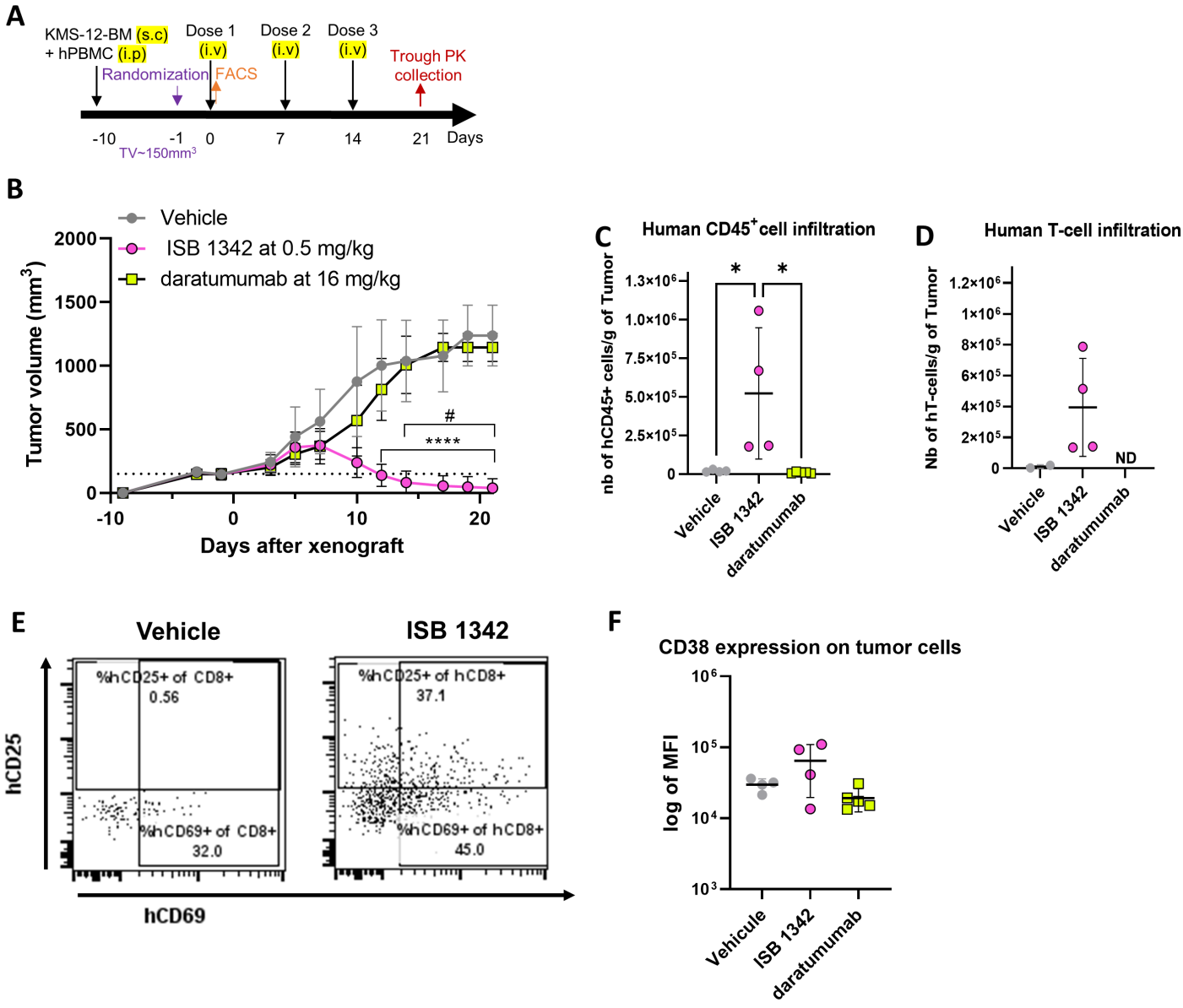
A
KMS-12-BM (s.c)
+ hPBMC (i.p)
Randomization
Dose 1 (i.v)
FACS
Dose 2 (i.v)
Dose 3 (i.v)
Trough PK collection
-10
-1
0
7
14
21
Days
TV~150mm3
B
Vehicle
ISB 1342 at 0.5 mg/kg
daratumumab at 16 mg/kg
Tumor volume (mm3)
Days after xenograft
#
****
C
Human CD45+cell infiltration
nb of hCD45+ cells/g of Tumor
Vehicle
ISB 1342
daratumumab
D
Human T-cell infiltration
Nb of hT-cells/g of Tumor
ND
E
Vehicle
ISB 1342
%hCD25+ of CD8+
0.56
%hCD69+ of CD8+
32.0
%hCD25+ of hCD8+
37.1
%hCD69+ of hCD8+
45.0
hCD25
hCD69
F
CD38 expression on tumor cells
log of MFI
Vehicule
ISB 1342
daratumumab

Figure 7

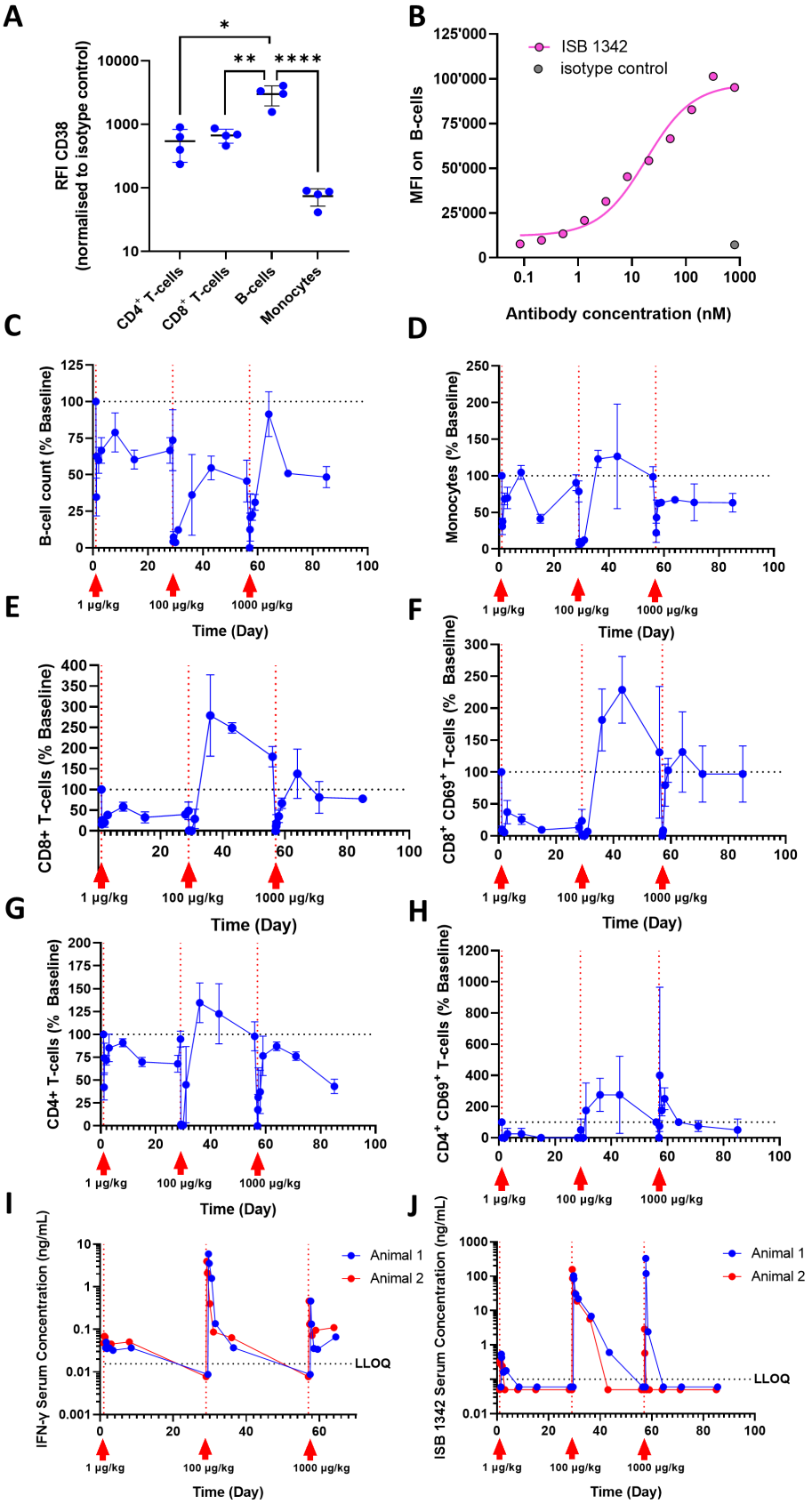
A
RFI CD38 (normalised to isotype control)
CD4+ T-cells
CD8+ T-cells
B-cells
Monocytes
B
ISB 1342
isotype control
MFI on B-cells
Antibody concentration (nM)
C
B-cell count (% Baseline)
D
Monocytes (% Baseline)
E
CD8+ T-cells (% Baseline)
F
CD8+ CD69+ T-cells (% Baseline)
G
CD4+ T-cells (% Baseline)
H
CD4+ CD69+ T-cells (% Baseline)
I
IFN-γ Serum Concentration (ng/mL)
J
ISB 1342 Serum Concentration (ng/mL)
Animal 1
Animal 2
LLOQ
1 µg/kg
100 µg/kg
1000 µg/kg
Time (Day)